# Bacterial Vaginosis Monitoring with Carbon

# Nanotube Field-effect Transistors

Zhengru Liu,<sup>†</sup> Long Bian,<sup>†</sup> Carl J. Yeoman,<sup>‡</sup> G. Dennis Clifton,<sup>±</sup> Joanna E. Ellington,<sup>±</sup> Rayne D. Ellington-Lawrence <sup>±</sup>, Joanna-Lynn C. Borgogna <sup>‡</sup> and Alexander Star<sup>†</sup> §\*

<sup>†</sup>Department of Chemistry, University of Pittsburgh, Pittsburgh, Pennsylvania 15260, USA

<sup>‡</sup>Departments of Microbiology and Cell Biology, and Animal and Range Sciences, Montana

State University, Bozeman, Montana 59718, USA

<sup>±</sup>Glyciome, LLC, Valleyford, Washington 99036 and Post Falls, Idaho 83854, USA

§Department of Bioengineering, University of Pittsburgh, Pittsburgh, Pennsylvania 15261, USA

Keywords: Rapid screening, carbon nanotubes, bacterial vaginosis, pH sensing, biogenic amines, machine learning, pregnancy

# **Abstract**

The ability to rapidly and reliably screen for bacterial vaginosis (BV) during pregnancy is of great significance for maternal health and pregnancy outcomes. In this proof-of-concept study, we demonstrated the potential of carbon nanotubes field-effect transistors (NTFET) in the rapid diagnostics of bacterial vaginosis with the sensing of BV-related factors such as pH and biogenic amines. The fabricated sensors showed good linearity to pH changes with a linear correlation coefficient of 0.99. The pH sensing

performance was stable after more than one month of sensor storage. In addition, the sensor was able to classify BV-related biogenic amine negative/positive samples with machine learning, utilizing different test strategies and algorithms, including linear discriminant analysis (LDA), support-vector machine (SVM), and principal component analysis (PCA). The biogenic amine sample status could be well classified using a soft-margin SVM model with a validation accuracy of 87.5%. The accuracy could be further improved using gold gate electrode for measurement, with accuracy higher than 90% in both LDA and SVM models. We also explored the sensing mechanisms and found that the change in NTFET off-current was crucial for classification. The fabricated sensors successfully detect BV-related factors, demonstrating the competitive advantage of NTFET for point-of-care diagnostics of BV.

# Introduction

Bacterial vaginosis (BV) represents a worldwide health issue, especially for pregnant women, as it is associated with an increased risk of obstetrical complications (e.g., premature membrane rupture, preterm birth and spontaneous abortion), sexually transmitted infections (e.g., HIV and human papillomavirus),<sup>1-6</sup> and some metabolic diseases during pregnancy such as preeclampsia and gestational diabetes.<sup>7-8</sup> The early and longitudinal awareness of BV during pregnancy is of great significance for improving maternal health and pregnancy outcomes. However, routine diagnostic methods for BV via clinical examinations (i.e., Amsel criteria) lack sensitivity to detect important underlying molecular changes associated with BV, even though one-third of pregnant women with BV are asymptomatic.<sup>9</sup> Other methods sufficient to identify asymptomatic BV, such as microscopy (i.e., Nugent criteria) or molecular diagnostics vary in their availability for women due to differences in healthcare access. Rapid point-of-care screening for the presence of BV-related biomolecules may provide an early indication of women at risk for BV-related pregnancy diseases regardless of symptomology.<sup>10</sup> Recent studies suggest the displacement of health-promoting vaginal bacteria (i.e., *Lactobacillus* spp.) and outgrowth of potential pathogenic bacteria are associated with increased levels of biochemicals known as biogenic amines (e.g., putrescine, cadaverine,

and tyramine) and elevated vaginal pH.<sup>11-13</sup> Consequently, women with BV-type microbiota are highly likely to retain at-risk bacterial populations throughout pregnancy, highlighting the importance of identifying these women early during gestation.<sup>14</sup> Figure S1 highlights the difference combined biogenic amine levels in vaginal samples from vaginal fluid samples of women who are clinically BV-negative and BV-positive.

Although other state-of-the-art analytical methods can determine biogenic amine levels, <sup>15-20</sup> access to BV diagnostics remains limited for self-testing and rapid, point-of-care settings, especially in populations with limited healthcare access. Current off-the-shelf patient tests for BV are limited to unreliable, color-change pH tests. <sup>21-22</sup> The measurement of biogenic amines is limited to the "Whiff" test in low-source settings, which is based on the odor due to the increased biogenic amines levels such as cadaverine and putrescine. However, the BV diagnostics with this subjective test are highly relied on the physicians' judgment, and the lack of access to odor testing equipment may increase the risk of BV misdiagnosis. An ideal, rapid point-of-care (POC) test kit for BV risk in women will require an adequate shelf-life, and sensitivity and specificity comparable to laboratory analytical instruments. <sup>9</sup> Additionally, manufacturing cost must allow commercial kit affordability across low-income and low-resource patients (e.g., Medicaid). Lastly, limited sensitivity and specificity of existing tests suggest that BV diagnostics may be optimized by using an array of sensors for parallel detections of different analytes rather than measurement of a single target molecule.

Biosensors based on carbon nanotubes make rapid screening of BV feasible by realizing monitoring of both vaginal pH and biogenic amines with the same sensor. Carbon nanotubes have been previously employed for pH sensing using optical techniques<sup>23-25</sup> and surface-enhanced Raman spectroscopy (SERS).<sup>26-27</sup> However, electrochemical detection methods have several advantages, including rapid analysis, high sensitivity, low cost of instrumentation, and outstanding advantages in miniaturization.<sup>28-31</sup> With the significant progress in microminiaturization and manufacturing cost control, fabricated electrochemical sensors show great potential in the point-of-care testing of pH. Different variables such as peak potential in voltammetry,<sup>32</sup> open circuit potential,<sup>33-35</sup> and resistance<sup>36</sup> can be employed for pH detection. Compared

with pH monitoring, the monitoring of physiologic biogenic amine levels requires a higher demand of electrochemical sensors. The stability of the sensor should be guaranteed to tolerate the complex sample matrix in the analysis, and the reuse of the sensor should be considered for cost control. In addition, the precise determination of biogenic amine compounds is difficult without separation techniques on the same electrochemical sensor, and the concentration of biogenic amines can vary widely between different samples. An electrochemical sensor with high specificity could be a solution for biogenic amines detection, but the bottleneck in muti-target analysis may limit its use since the BV diagnostics could not be determined by a single type of biogenic amine compound. And in fact, the construction of a sensor with high specificity may lead to the increased cost and workload in the device production due to extra labeling/blocking steps, which is not affordable for low-income and low-resource patient screens of BV-risk (i.e., at-risk or low-risk).

Diagnostic modalities that qualitatively test for BV presence in biologic samples based on a combination of related factors including increased pH and a relative change in biogenic amine levels may be superior as a point-of-care diagnostic test compared to precise quantification methods such as fluorescence spectroscopy<sup>18</sup> or mass spectrometry.<sup>19</sup> Fabrication of sensors that classify BV sample type may also be more straightforward, user-friendly, and accurate for women across differing racial groups, reproductive-stages and ages (all of which can impact baseline vaginal measurements). Machine learning has been applied previously as a powerful tool to classify sample types. Our previous studies have correctly classified different purine compounds/volatile organic compounds/metal ions with NTFET biosensors.<sup>37-39</sup> The interactions between analytes and NTFET could result in the different changes of the transfer characteristics, which are extracted as different features in the training model. The "fingerprints" of different BV types (e.g., BV-negative versus BV-positive) composed of these features could be classified with the machine learning method. However, the concentrations of diagnostically important compounds differ significantly across biological samples from different BV patients, making accurate classification of these samples more difficult than samples with fixed concentrations. The complexity of biological matrix

also results in large uncertainty, for which an optimized protocol should be developed to make the measurement more reliable.

Herein, we aimed to realize both pH sensing and biogenic amine classification with the same sensor. The integration of multiple devices on the same sensor chip improves its potential capacity for monitoring different diagnostic targets. To this end, firstly, NTFET devices with different decorations were fabricated and tested for pH sensing. We then evaluated the pH sensing results from the 1st to 33rd days. The NTFET devices decorated with gold nanoparticles (Au-NTFET) were considered a favorite choice with a shelf-life of more than one month. The Au-NTFET devices were then used for the classification of biogenic amines across a range of sample concentration (mimicking BV-positive and BV-negative samples). Both Ag/AgCl and Au reference electrodes were tested as liquid gate electrodes in the NTFET measurements. The accuracy of different machine learning training models was explored using different algorithms such as linear discriminant analysis, linear support-vector machine (both hard-margin and soft-margin), and principal component analysis (PCA). The BV negative/positive samples were well classified with the optimized test protocol. The accuracy value was higher than 90%, showing the feasibility of NTFET for POC diagnostics of BV.

# **Materials and Methods**

Carbon Nanotube-based Field-Effect Transistor (NTFET) Fabrication. The  $2 \times 2 \text{ mm}^2$  Si/SiO<sub>2</sub> wafers with four interdigitated gold electrodes were fabricated using photolithography. After being wire-bonded into 40-pin ceramic dual-inline packages (CERDIP), the chips were secured with polydimethylsiloxane (PDMS) by heating at 80 °C for 1 h. The semiconducting single-walled carbon nanotubes (IsoSol-SWCNTs) were deposited on the chips using dielectrophoresis (DEP) with a Keithley 3390 Arbitrary Waveform. The 3  $\mu$ L of IsoSol-SWCNTs (0.02 g mL<sup>-1</sup>, dispersed in toluene, NanoIntegris) were deposited between the gold electrodes with a bias voltage of 10 V and a frequency of 100 Hz for 2 min. The packages were annealed at 120 °C overnight. Then carbon nanotubes were decorated with gold

nanoparticles through bulk electrolysis of HAuCl<sub>4</sub> (HAuCl<sub>4</sub>·3H<sub>2</sub>O, Alfa Aesar) solution at -0.2 V for 30 s using a 3-electrodes system (Reference: 1 M Ag/AgCl electrode; Counter: Pt electrode; Working: interdigitated gold electrodes with carbon nanotubes). Lastly, the gold nanoparticles were functionalized with different self-assembled monolayers (SAM). 200  $\mu$ L of dodecanethiol (10 mM, V<sub>ethanol</sub>/V<sub>water</sub> = 1:1, Sigma-Aldrich) and 11-mercaptoundecanoic acid (10 mM, V<sub>ethanol</sub>/V<sub>water</sub> = 7:3, Sigma-Aldrich) were separately incubated on the chips for 2 and 24 h to fabricate different types of sensors. The chips were washed with ethanol and deionized water after functionalization and dried for the following tests.

**Electrical Measurements**. The NTFET characteristics were measured using two different source meters, Keithley Source Meter Unit 2400 and 2602B. A 1 M Ag/AgCl electrode (CH Instruments, Inc.) was used as the gate electrode in both pH sensing and biogenic amines detection. The gate voltage ( $V_g$ ) was swept from +0.6 V to -0.6 V with a source-drain voltage ( $V_{sd}$ ) of 0.05 V in the measurement. An Au electrode (CH Instruments, Inc.) was also used as the liquid gate electrode to detect the biogenic amines.

pH Sensing on Different Sensors. The scheme of pH/biogenic amines sensing is shown in Figure 1. pH buffers from 2 to 12 were prepared based on the Britton-Robinson methods.<sup>40</sup> Solution of H<sub>3</sub>PO<sub>4</sub>, H<sub>3</sub>BO<sub>3</sub>, and CH<sub>3</sub>COOH (0.04 M) were prepared by dissolving the acids in 100 mL of water with an initial pH of ~1.8. The buffers from pH 2 to 12, with increments of one, were prepared by adding 0.2 M of NaOH solution. A Mettler Toledo Seven Multi pH meter was employed for the measurement of pH.

The prepared devices were firstly immersed in 400  $\mu$ L of buffer (pH =12) for 1 h to reach the balance in the ion transfer between the functionalized carbon nanotubes and the buffer. After the rinsing step, the devices were immersed in another 400  $\mu$ L of buffer (pH = 12) for 5 minutes, and NTFET characteristics were measured. The FET measurements were repeated every 5 minutes until NTFET characteristics were constant. Subsequently, the devices were immersed in the buffers with pH values from 12 to 2 successively, and NTFET characteristics were measured after 5 minutes. Between the switch of buffers, both devices and gate electrodes were rinsed with deionized water. The NTFET characteristics were also measured in the buffers in reverse order from pH 2 to 12.

Biogenic Amines Sensing. Sensing with Ag/AgCl Gate Electrode. An artificial vaginal fluid simulant (VFS) was prepared following the previously reported recipe<sup>41</sup> and inoculated with physiologically-relevant concentrations of the biogenic amines putrescine, cadaverine, spermine, spermidine, and tyramine as reported in the previous publication,<sup>12</sup> as well as agmatine and trimethylamine that were measured from the same sample set as the publication<sup>12</sup> and are shown in Table S1. Median biogenic amine concentrations from samples classified as BV-negative and median concentrations from the samples classified as BV-negative and BV-positive mock samples. Before the test, the devices were immersed in deionized water firstly until the NTFET characteristics were constant. In the sensing process, the devices were incubated with 400 μL of deionized water for 10 min, and NTFET characteristics were measured as the control group. Subsequently, the devices were incubated with 400 μL of BV negative/positive samples for another 10 min, and NTFET characteristics were measured as the test group. To collect NTFET characteristics, the devices were rinsed with deionized water after incubation, and NTFET characteristics were measured in 0.01 M phosphate buffer (PBS).

Sensing with Au Gate Electrode. In the sensing process with the Au gate electrode, the Au electrode was immersed in the solution directly during the test. The devices were incubated with 400 μL of PBS for 10 min, and NTFET characteristics were measured directly as the control group without the rinsing step. The devices were then immersed in 400 μL of BV negative/positive samples for another 10 min, and NTFET characteristics were measured as the test group. Before the following sample test, the Au electrode was rinsed with acetone, isopropanol, and deionized water.

**Data Processing**. For each sample, the features calculations were based on the NTFET characteristics from the test and control groups. Based on our previously published work's established machine learning strategy, <sup>42</sup> 15 features were extracted from the transfer characteristics (Figure S2 and Table S2), and different LDA/SVM models were selected for classification using Python 3.7 (Table S3). Past 3 software was used for the visualization of results in the LDA model. The elimination of features was based on recursive feature elimination with a cross-validation (k=10) method.

#### **Results and Discussion**

pH Sensing. The fabricated sensors were tested for pH sensing within the range of pH values between 2 and 12. It has been previously reported that carbon nanotubes are highly sensitive to pH changes, and NTFET devices have been applied for pH sensing. 43-46 Because the sensors with different decorations may respond to the pH changes differently due to the different functional groups, the NTFET characteristics at different pH values were investigated on the NTFETs decorated with gold nanoparticles (Au-NTFET), and after functionalization with dodecanethiol SAMs (DD-NTFET) and 11-mercaptoundecanoic acid SAMs (MUA-NTFET). The dodecanethiol SAMs provide a hydrophobic interface and the 11-mercaptoundecanoic acid SAMs are hydrophilic. The sensors with bare carbon nanotubes were also tested.

Before testing, each device was immersed in a buffer (pH 12) to balance the interactions between hydronium ions and carbon nanotubes. Subsequently, the NTFET characteristics, i.e., source-drain current versus applied liquid gate voltage, at different pH values were measured. As shown in Figure 2 (pH 12 to 2) and Figure S3 (pH 2 to 12), the drain current decreased with the decrease of pH, and the threshold voltage shifted to the negative direction. The negative shift in pH sensing indicated that the doping mechanism might be a general one in different sensing applications with our fabricated sensors. We observed the decrease of current at –0.6 V (associated with on-current) but increase of current at 0.6 V (associated with off-current). The opposite trend in off-current changes might indicate a contribution from other sensing mechanisms such as Schottky barrier modulation.<sup>47</sup> To investigate the influence of solvent, the NTFET characteristics at different pH values were measured in two opposite test sequences (From 12 to 2 and 2 to 12 in turn), and similar results were obtained, showing that the current changes were only related to pH changes.

We also evaluated the linearity between the device conductance and pH values based on the conductance values at -0.5 V. As shown in Figure 3, good linearity was obtained for all four sensor types with linear correlation coefficients between 0.97 and 0.99. The results showed the capacity of fabricated sensors in pH sensing in a wide pH range (2 to 12). It should be noted that the good linearity could always be observed regardless of the decoration strategies, suggesting that the hydronium ions might interact with

carbon nanotubes directly in the sensing process. The defects on sidewalls of bare carbon nanotubes, the wrapped polymer used to enrich the semiconducting CNTs, and the SiO<sub>2</sub>/Si chip surface might also participate in this process. We also investigated the shelf-life of our fabricated sensors after storage at room temperature. The results for Au-NTFET (Figure S4) showed that the sensitivity remains unchanged after storage for 12 days, and the sensors still demonstrated pH sensing after 33 days with a linear correlation coefficient of 0.99 (Figure 3b, albeit at lower conductance values), suggesting that the fabricated sensors have an acceptable shelf-life. We also investigated the shelf-life of three other sensor types but found them inferior to Au-NTFET (Figure S5).

Biogenic Amines Sensing. Sensing with Ag/AgCl Electrode. Because of their long shelf-life in pH sensing, the sensors decorated with bare gold nanoparticles (Au-NTFET) were chosen for the biogenic amines sensing evaluation. These sensors, after storage for different time lengths, were randomly chosen for the following studies. A 1 M Ag/AgCl electrode was employed as the liquid gate electrode for the investigation. Considering about the low stability of some biogenic amines such as tyramine, the VFS control was applied to prepare the BV-negative and BV-positive mock samples, given that innate buffering capability of vaginal secretions (e.g., lactate/lactic acid) or addition of exogenous buffers may act to stabilize biogenic amines over time. 48 For both negative and positive samples, the conductance decrease could be observed after sample incubation (Figures 4a and b). The conductance decrease indicated that some biomolecules might be adsorbed on the devices after incubation and result in the changes of NEFET characteristics. We also measured the NTFET characteristics after incubation with VFS controls (without biogenic amines). The conductance increased slightly after incubation (Figure S6), indicating that any conductance decrease was only related to the interaction between biogenic amines and CNT hybrids. However, the classification of BV-negative/positive samples could not be achieved based on the conductance changes alone because there were no significant differences between outcomes in these two groups. Machine learning techniques were then applied for the classification based on the 15 features extracted from the NTFET characteristics. These 15 features were selected based on the transfer characteristics of field-effect transistors, such as the transconductance change in the linear region, the

changes of conductance values at different voltages, and the shift of threshold voltage. These feature values are associated with different sensing mechanisms such as doping mechanism and Schottky barrier modulation, <sup>47, 49-52</sup> which can explain the interactions between the compounds and the CNT. Both linear discriminant analysis (LDA) and support-vector machine (SVM) were employed as algorithms in model training. However, the results showed that the validation accuracy values were only about 68.0% for the LDA model and 52.0% for the SVM model (Figure S7 and Tables S4-S5). The training accuracy values (85.0% for the LDA model and 62.8% for the SVM model) were also unsatisfactory, which were insufficient for sample classification.

Optimization of Training Model. The low accuracy indicated that the model required optimization for classification. We tried to optimize the model based on different combinations of the features. Based on the characteristics of NTFET devices fabricated from semiconducting SWCNTs, we discarded some features to simplify the model in the first step. Eight features, including Features 1, 2, 5, 7, 9, 11, 13, and 15 were selected, which represented the transconductance changes, threshold voltage changes, and conductance changes in the linear region. However, some of these features might be correlated to each other, given that all the conductance values were picked from the linear region. Therefore, Pearson correlation coefficient values were calculated for the evaluation of correlations among the selected eight features. The results in Figure S8 showed that only Feature 2 was uncorrelated to other features. All the features related to conductance changes (Feature 5 to 15) were highly related to each other, and Feature 1 (transconductance changes) was also related to the conductance changes, indicating that more features could be eliminated from the model. One-way ANOVA was then used to compare each feature between the BV-negative and BV-positive sample groups. The results in Table S7 showed that Feature 1 and Feature 2 were significantly different in these two groups, indicating that these two might be critical features for sample classification. The p-values of all the other features were higher than 0.8, which means that the classification might not be realized with conductance changes alone.

Since Feature 2 was the only one which was not related to other features and significantly different in the BV-negative/positive samples, the distribution of Feature 2 was studied. In the data set, the samples

were split as training group and test group randomly with a ratio of 4:1. However, the training accuracy (64.4%) was still not good (shown in the confusion matrix in Table S5), but a high validation accuracy (87.5%) was obtained in the test group even with such a training set. Herein, soft-margin SVM was applied as the algorithm for the sample classification, which maximized the margin but still allowed some misclassifications within it. We chose three features for the classification in this model. Besides Feature 1 and Feature 2, Feature 8 was also kept in the model because a relatively low p-value was obtained for Feature 8 in one-way ANOVA. The confusion matrix in Table S5 showed that high accuracy could be obtained in both the training group (89.8%) and the test group (87.5%) using these selected features. The validation accuracy was comparable to training accuracy, showing the robustness of the model. In addition, it was also comparable with the validation accuracy in the test group with LDA.

In summary, the BV-negative/positive samples were well classified using soft-margin SVM after optimizing the model with the elimination of features. The accuracy could be significantly improved with the selection of features and algorithms. However, a higher accuracy was desired, and the errors in the classification could not be ignored. This strategy assumed that the biogenic amines molecules would be irreversibly adsorbed on the SWCNT devices. Because of the differences in biogenic amine concentrations between BV-negative and BV-positive samples, different NTFET characteristics could be observed and discriminated with the developed model. However, the results showed that these biomolecules might be washed away according to the recovery of drain current after several washing steps (Figure S9). The loss of biomolecules after washing might offset the differences in the concentrations between BV-negative and BV-positive samples, potentially resulting in the low accuracy in the classification.

Sensing with Au Electrode. The NTFET characteristics were measured directly after incubation without rinsing in order to eliminate the influence of the rinsing step. The gate electrode was immersed in the sample solution during the whole incubation process. However, we found that the Ag/AgCl electrode could not tolerate the matrix, leading to no response to the sample solution. Therefore, we chose the Au electrode as the gate electrode for the investigation. As shown in Figures 4c and d, the Au electrode can be used to detect both BV-negative and BV-positive sample types. Compared with the NTFET characteristics

with Ag/AgCl electrode, the threshold voltage was even more positive with the Au electrode. The threshold voltage was around 0.1 V in the phosphorate buffer with the Ag/AgCl electrode, but around 0.5 V with the Au electrode. Meanwhile, a higher off-current could be observed (0.1 to 5 μA with the Ag/AgCl electrode versus 5 to 20 μA with Au electrode). We also investigated the adsorption of biogenic amine molecules on the Au electrode. The repeatable NTFET characteristics in two tests (Figure S10) showed that these biomolecules could be thoroughly washed away after incubation, which guaranteed the reuse of Au electrodes on different sensors.

With the same 15 features, both LDA and SVM models were used to classify BV negative and positive samples. As shown in Figure 5a and Tables S4-S5, the two groups could be well classified using Au electrode with a training/validation accuracy of 100% in both models, indicating the significant improvement of accuracy with the change of gate electrode. Principal component analysis (PCA) was also applied for data training, and BV-negative/positive samples were also well classified in the PCA model. The high accuracy of the PCA model (Figure 5b) supported our hypothesis given that the two groups were not classified in advance in an unsupervised learning method. Lastly, we used the recursive feature elimination with cross-validation (RFECV) method to investigate the crucial features in the classification in both the LDA and SVM models. <sup>38</sup> The results in Figure S11 and Table S8 indicated that only 3 of 15 features in the LDA model could achieve a validation accuracy of 100%. For the linear-SVM model, only one feature was enough for the validation accuracy of 100%. The result from RFECV-SVM showed that Feature 14 was dominant in the classification, which represented the off-current change. In the RFECV-LDA model, on-current change (Feature 15) and transconductance (Feature 1) also contributed to the classification as well as the off-current change (Feature 8). Herein, we could conclude that the off-current change might dominate the classification of biogenic amine samples with a gold liquid gate electrode, consistent with the opposite changes in off-current for the negative and positive samples shown in Figure 4. The off-current would decrease after sample incubation in negative samples, but remain the same or even increase, after incubation in most positive samples, showing as the difference in values of features in Figure S12. The off-current changes were also accompanied by a threshold voltage shift, demonstrating that the

doping mechanism might play a key role in biogenic amine sensing. In addition, the transconductance changes should also be considered, indicating the contributions of other sensing mechanisms.

#### Conclusion

We successfully demonstrated the application of NTFET in the rapid screening of mock bacterial vaginosis samples (i.e. BV-negative or BV-positive), realized by pH sensing and biogenic amine classification using the same carbon nanotube-based sensor. Four types of NTFET sensors based on different decorations were fabricated, and all of them showed strong linearity with high linear correlation coefficients (0.97 to 0.99) in pH sensing. Acceptable prototype stability was observed on the carbon nanotube sensor decorated with bare gold nanoparticles (Au-NTFET) after storing at room temperature for one month, which was fundamental to applying carbon nanotube sensors in the proposed POC BVdiagnostic. The Au-NTFET sensor was also used to classify biogenic amine levels in samples, reflecting "healthy" (BV-negative) and "diseased" (BV-positive) sample types with machine learning techniques to optimize training models and testing strategy. In addition, the cost of each fabricated sensor is low (e.g., ~\$1/sensor), and time-efficient (e.g., 15 minutes/sensor), although prototype design is still under optimization, batch production over days is possible. With the introduction of the materials printing techniques and an automated system, it is expected that mass production of sensors and a low cost of each test could make this device accessible to low-income and low-resource patients and POC healthcare providers. Despite the demonstrated high accuracy, this remains a proof-of-concept study conducted on mock samples. Additional work is needed to assess the sensor performance across the breadth of biogenic amine concentrations documented among human samples<sup>12</sup> and in a background of the many other common vaginal biomolecules,53 both of which may affect the accurate classification of BV. The complex and dynamic vaginal metabolic profile will require further sensor development for the rapid screening of bacterial vaginosis, with refinement of a diagnostic test to screen for bacterial vaginosis in patient samples (including greater compound and factor diversity). In addition, a standard operating procedure need to be

established for the quality control of samples in the collection, transportation, storage, and testing to eliminate the errors from operations.

Additionally, the design of a portable electronic unit instead of the laboratory analytical instruments used in this work should be accomplished for successful POC or user-based diagnostics. More data is needed to construct a general model in the rapid screening of BV with machine learning. This will be further explored in our future work. The current study demonstrated the feasibility of using a NEFET device in conjunction with different machine learning models to qualitatively classify mock BV biologic samples accurately. Further refinement and development of the technology may provide an economical, minimally invasive, rapid POC test for women in low-resource healthcare settings, poised to significantly decrease BV prevalence in at-risk populations.

# **Supporting Information**

NTFET characteristics of different devices in different tests; Feature extraction methods; Shelf life of different sensors in pH sensing; Results in quantification with LC-MS; Results of statistical analysis; LDA and SVM plots; Confusion matrices.

# Acknowledgements

This work is supported by the National Science Foundation under grant no. 2003302 and by gifts by Glyciome, LLC.

### **Author Information**

# **Corresponding Author**

Alexander Star — Department of Chemistry and Department of Bioengineering, University of Pittsburgh, Pittsburgh, Pennsylvania 15260, United States; orcid.org/0000-0001-7863-5987; Email: astar@pitt.edu

#### **Authors**

**Zhengru Liu** — Department of Chemistry, University of Pittsburgh, Pittsburgh, Pennsylvania 15260, United States

**Long Bian** — Department of Chemistry, University of Pittsburgh, Pittsburgh, Pennsylvania 15260, United States

Carl J. Yeoman — Department of Range and Animal Sciences, Montana State University, Bozeman, Montana 59718, United States

**G. Dennis Clifton** — Glyciome, LLC, Valleyford, Washington 99036, and Post Falls, Idaho 83854, United States

**Joanna E. Ellington** — Glyciome, LLC, Valleyford, Washington 99036, and Post Falls, Idaho 83854, United States

R.D. Ellington-Lawrence — Glyciome, LLC, Valleyford, Washington 99036, and Post Falls, Idaho 83854, United States

# References

- 1. Kinuthia, J.; Drake, A. L.; Matemo, D.; Richardson, B. A.; Zeh, C.; Osborn, L.; Overbaugh, J.; McClelland, R. S.; John-Stewart, G., HIV acquisition during pregnancy and postpartum is associated with genital infections and partnership characteristics. *Aids* **2015**, *29* (15), 2025-2033.
- 2. Kero, K.; Rautava, J.; Syrjanen, K.; Grenman, S.; Syrjanen, S., Association of asymptomatic bacterial vaginosis with persistence of female genital human papillomavirus infection. *Eur. J. Clin. Microbiol. Infect. Dis.* **2017**, *36* (11), 2215-2219.
- 3. Grewal, K.; MacIntyre, David A.; Bennett, Phillip R., The reproductive tract microbiota in pregnancy. *Biosci. Rep.* **2021**, *41* (9).
- 4. van de Wijgert, J.; Jespers, V., The global health impact of vaginal dysbiosis. *Res. Microbiol.* **2017**, *168* (9-10), 859-864.
- 5. Chen, X. D.; Lu, Y. N.; Chen, T.; Li, R. G., The Female Vaginal Microbiome in Health and Bacterial Vaginosis. *Front. Cell. Infect. Microbiol.* **2021**, *11*.
- 6. Redelinghuys, M. J.; Geldenhuys, J.; Jung, H.; Kock, M. M., Bacterial Vaginosis: Current Diagnostic Avenues and Future Opportunities. *Front. Cell. Infect. Microbiol.* **2020**, *10*.
- 7. Cortez, R. V.; Taddei, C. R.; Sparvoli, L. G.; Angelo, A. G. S.; Padilha, M.; Mattar, R.; Daher, S., Microbiome and its relation to gestational diabetes. *Endocrine* **2019**, *64* (2), 254-264.
- 8. Lin, C. Y.; Lin, C. Y.; Yeh, Y. M.; Yang, L. Y.; Lee, Y. S.; Chao, A.; Chin, C. Y.; Chao, A. S.; Yang, C. Y., Severe preeclampsia is associated with a higher relative abundance of Prevotella bivia in the vaginal microbiota. *Sci. Rep.* **2020**, *10* (1), 13.

- 9. *Bacterial Vaginosis*; Centers for Disease Control and Prevention, 2021. <a href="https://www.cdc.gov/std/treatment-guidelines/bv.htm">https://www.cdc.gov/std/treatment-guidelines/bv.htm</a> (accessed October 23, 2021).
- 10. Saweri, O. P. M.; Batura, N.; Al Adawiyah, R.; Causer, L. M.; Pomat, W. S.; Vallely, A. J.; Wiseman, V., Economic evaluation of point-of-care testing and treatment for sexually transmitted and genital infections in pregnancy in low- and middle-income countries: A systematic review. *PLOS ONE* **2021**, *16* (6), e0253135.
- 11. Owens, D. K.; Davidson, K. W.; Krist, A. H.; Barry, M. J.; Cabana, M.; Caughey, A. B.; Donahue, K.; Doubeni, C. A.; Epling, J. W.; Kubik, M.; Ogedegbe, G.; Pbert, L.; Silverstein, M.; Simon, M. A.; Tseng, C. W.; Wong, J. B.; Force, U. S. P. S. T., Screening for Bacterial Vaginosis in Pregnant Persons to Prevent Preterm Delivery US Preventive Services Task Force Recommendation Statement. *JAMA* **2020**, *323* (13), 1286-1292.
- 12. Borgogna, J. L. C.; Shardell, M. D.; Grace, S. G.; Santori, E. K.; Americus, B.; Li, Z.; Ulanov, A.; Forney, L.; Nelson, T. M.; Brotman, R. M.; Ravel, J.; Yeoman, C. J., Biogenic Amines Increase the Odds of Bacterial Vaginosis and Affect the Growth of and Lactic Acid Production by Vaginal Lactobacillus spp. *Appl. Environ. Microbiol.* **2021**, *87* (10).
- 13. Puebla-Barragan, S.; Akouris, P. P.; Al, K. F.; Carr, C.; Lamb, B.; Sumarah, M.; van der Veer, C.; Kort, R.; Burton, J.; Reid, G., The Two-Way Interaction between the Molecules That Cause Vaginal Malodour and Lactobacilli: An Opportunity for Probiotics. *International Journal of Molecular Sciences* **2021**, *22* (22), 12279.
- 14. Serrano, M. G.; Parikh, H. I.; Brooks, J. P.; Edwards, D. J.; Arodz, T. J.; Edupuganti, L.; Huang, B.; Girerd, P. H.; Bokhari, Y. A.; Bradley, S. P.; Brooks, J. L.; Dickinson, M. R.; Drake, J. I.; Duckworth, R. A.; Fong, S. S.; Glascock, A. L.; Jean, S.; Jimenez, N. R.; Khoury, J.; Koparde, V. N.; Lara, A. M.; Lee, V.; Matveyev, A. V.; Milton, S. H.; Mistry, S. D.; Rozycki, S. K.; Sheth, N. U.; Smirnova, E.; Vivadelli, S. C.; Wijesooriya, N. R.; Xu, J.; Xu, P.; Chaffin, D. O.; Sexton, A. L.; Gravett, M. G.; Rubens, C. E.; Hendricks-Muñoz, K. D.; Jefferson, K. K.; Strauss, J. F.; Fettweis, J. M.; Buck, G. A., Racioethnic diversity in the dynamics of the vaginal microbiome during pregnancy. *Nat. Med.* **2019**, *25* (6), 1001-1011.
- 15. Onal, A., A review: Current analytical methods for the determination of biogenic amines in foods. *Food Chem.* **2007**, *103* (4), 1475-1486.
- 16. Sun, X. H.; Yang, X. R.; Wang, E. K., Determination of biogenic amines by capillary electrophoresis with pulsed amperometric detection. *J. Chromatogr. A* **2003**, *1005* (1-2), 189-195.
- 17. Liu, Y. M.; Cheng, J. K., Separation of biogenic amines by micellar electrokinetic chromatography with on-line chemiluminescence detection. *J. Chromatogr. A* **2003**, *1003* (1-2), 211-216.
- 18. Cao, L. W.; Wang, H.; Ma, M.; Zhang, H. S., Determination of biogenic amines in HeLa cell lysate by 6-oxy-(N-succinimidyl acetate)-9-(2 '-methoxycarbonyl) fluorescein and micellar electrokinetic capillary chromatography with laser-induced fluorescence detection. *Electrophoresis* **2006**, *27* (4), 827-836.
- 19. Diesner, M.; Neupert, S., Quantification of Biogenic Amines from Individual GFP-Labeled Drosophila Cells by MALDI-TOF Mass Spectrometry. *Anal. Chem.* **2018**, *90* (13), 8035-8043.
- 20. Lerga, T. M.; Jauset-Rubio, M.; Skouridou, V.; Bashammakh, A. S.; El-Shahawi, M. S.; Alyoubi, A. O.; O'Sullivan, C. K., High Affinity Aptamer for the Detection of the Biogenic Amine Histamine. *Anal. Chem.* **2019**, *91* (11), 7104-7111.
- 21. Monaghan, M. T.; Brogan, K.; Lockington, D.; Rotchford, A. P.; Ramaesh, K., Variability in measuring pH using litmus paper and the relevance in ocular chemical injury. *Eye* **2020**, *34* (11), 2133-2134.
- 22. Connor, A. J.; Severn, P., Use of a control test to aid pH assessment of chemical eye injuries. *Emerg Med J* **2009**, *26* (11), 811-812.
- Zhao, W.; Song, C. H.; Pehrsson, P. E., Water-soluble and optically pH-sensitive single-walled carbon nanotubes from surface modification. *J. Am. Chem. Soc.* **2002**, *124* (42), 12418-12419.
- 24. Cho, E. S.; Hong, S. W.; Jo, W. H., A New pH Sensor Using the Fluorescence Quenching of Carbon Nanotubes. *Macromol. Rapid Commun.* **2008**, *29* (22), 1798-1803.

- 25. Kulkarni, M. V.; Charhate, N. A.; Bhavsar, K. V.; Tathe, M. A.; Kale, B. B., Development of polyaniline-multiwalled carbon nanotube (PANI-MWCNT) nanocomposite for optical pH sensor. *Mater. Res. Innov.* **2013**, *17* (4), 238-243.
- 26. Zhao, L.; Shingaya, Y.; Tomimoto, H.; Huang, Q.; Nakayama, T., Functionalized carbon nanotubes for pH sensors based on SERS. *J. Mater. Chem.* **2008**, *18* (40), 4759-4761.
- 27. Chen, P.; Wang, Z. Y.; Zong, S. F.; Chen, H.; Zhu, D.; Zhong, Y.; Cui, Y. P., A wide range optical pH sensor for living cells using Au@Ag nanoparticles functionalized carbon nanotubes based on SERS signals. *Anal. Bioanal. Chem.* **2014**, *406* (25), 6337-6346.
- 28. Kim, S. N.; Rusling, J. F.; Papadimitrakopoulos, F., Carbon nanotubes for electronic and electrochemical detection of biomolecules. *Adv. Mater.* **2007**, *19* (20), 3214-3228.
- 29. Jacobs, C. B.; Peairs, M. J.; Venton, B. J., Review: Carbon nanotube based electrochemical sensors for biomolecules. *Anal. Chim. Acta* **2010**, *662* (2), 105-127.
- 30. Wang, Z. H.; Yu, J. B.; Gui, R. J.; Jin, H.; Xia, Y. Z., Carbon nanomaterials-based electrochemical aptasensors. *Biosens. Bioelectron.* **2016**, *79*, 136-149.
- 31. Ziegler, J. M.; Andoni, I.; Choi, E. J.; Fang, L.; Flores-Zuleta, H.; Humphrey, N. J.; Kim, D. H.; Shin, J.; Youn, H.; Penner, R. M., Sensors Based Upon Nanowires, Nanotubes, and Nanoribbons: 2016-2020. *Anal. Chem.* **2021**, *93* (1), 124-166.
- 32. Wildgoose, G. G.; Leventis, H. C.; Streeter, I.; Lawrence, N. S.; Wilkins, S. J.; Jiang, L.; Jones, T. G. J.; Compton, R. G., Abrasively immobilised multiwalled carbon nanotube agglomerates: A novel electrode material approach for the analytical sensing of pH. *ChemPhysChem* **2004**, *5* (5), 669-677.
- 33. Xu, B.; Zhang, W. D., Modification of vertically aligned carbon nanotubes with RuO2 for a solid-state pH sensor. *Electrochim. Acta* **2010**, *55* (8), 2859-2864.
- 34. Li, C. A.; Han, K. N.; Pham, X. H.; Seong, G. H., A single-walled carbon nanotube thin film-based pH-sensing microfluidic chip. *Analyst* **2014**, *139* (8), 2011-2015.
- 35. Qin, Y. H.; Kwon, H. J.; Subrahmanyam, A.; Howlader, M. M. R.; Selvaganapathy, P. R.; Adronov, A.; Deen, M. J., Inkjet-printed bifunctional carbon nanotubes for pH sensing. *Mater. Lett.* **2016**, *176*, 68-70.
- 36. Goh, G. L.; Agarwala, S.; Tan, Y. J.; Yeong, W. Y., A low cost and flexible carbon nanotube pH sensor fabricated using aerosol jet technology for live cell applications. *Sens. Actuator B-Chem.* **2018**, *260*, 227-235.
- 37. Hwang, S. I.; Franconi, N. G.; Rothfuss, M. A.; Bocan, K. N.; Bian, L.; White, D. L.; Burkert, S. C.; Euler, R. W.; Sopher, B. J.; Vinay, M. L.; Sejdic, E.; Star, A., Tetrahydrocannabinol Detection Using Semiconductor-Enriched Single-Walled Carbon Nanotube Chemiresistors. *ACS Sens.* **2019**, *4* (8), 2084-2093.
- 38. Bian, L.; Sorescu, D. C.; Chen, L.; White, D. L.; Burkert, S. C.; Khalifa, Y.; Zhang, Z.; Sejdic, E.; Star, A., Machine-Learning Identification of the Sensing Descriptors Relevant in Molecular Interactions with Metal Nanoparticle-Decorated Nanotube Field-Effect Transistors. *ACS Appl. Mater. Interfaces* **2019**, *11* (1), 1219-1227.
- 39. Bian, L.; Wang, Z.; White, D. L.; Star, A., Machine learning-assisted calibration of Hg<sup>2+</sup> sensors based on carbon nanotube field-effect transistors. *Biosens. Bioelectron.* **2021**, *180*, 113085.
- 40. Britton, H. T. S.; Robinson, R. A., CXCVIII.—Universal buffer solutions and the dissociation constant of veronal. *J. Chem. Soc. (Resumed)* **1931**, (0), 1456-1462.
- 41. Rastogi, R.; Su, J.; Mahalingam, A.; Clark, J.; Sung, S.; Hope, T.; Kiser, P. F., Engineering and characterization of simplified vaginal and seminal fluid simulants. *Contraception* **2016**, *93* (4), 337-346.
- 42. Silva, G. O.; Michael, Z. P.; Bian, L.; Shurin, G. V.; Mulato, M.; Shurin, M. R.; Star, A., Nanoelectronic Discrimination of Nonmalignant and Malignant Cells Using Nanotube Field-Effect Transistors. *ACS Sens.* **2017**, *2* (8), 1128-1132.
- 43. Huang, B. R.; Lin, T. C., Leaf-like carbon nanotube/nickel composite membrane extended-gate field-effect transistors as pH sensor. *Appl. Phys. Lett.* **2011**, *99* (2), 3.

- 44. Gou, P.; Kraut, N. D.; Feigel, I. M.; Bai, H.; Morgan, G. J.; Chen, Y.; Tang, Y.; Bocan, K.; Stachel, J.; Berger, L.; Mickle, M.; Sejdić, E.; Star, A., Carbon Nanotube Chemiresistor for Wireless pH Sensing. *Sci. Rep.* **2014**, *4* (1), 4468.
- 45. Doroodmand, M. M.; Nemati, Y.; Mohebbi-Fani, M., Specific pH Sensor Based on Nitrogen/Carbon Nanotube-Modified Commercial Field-Effect Transistor for Detection of Rumen pH in Ruminants In Situ. *IEEE Sens. J.* **2016**, *16* (9), 2906-2913.
- 46. Chen, X.; Zhang, H. N.; Tunuguntla, R. H.; Noy, A., Silicon Nanoribbon pH Sensors Protected by a Barrier Membrane with Carbon Nanotube Porins. *Nano Lett.* **2019**, *19* (2), 629-634.
- 47. Heller, I.; Janssens, A. M.; Mannik, J.; Minot, E. D.; Lemay, S. G.; Dekker, C., Identifying the mechanism of biosensing with carbon nanotube transistors. *Nano Lett.* **2008**, *8* (2), 591-595.
- 48. Eugster, P. J.; Centeno, C.; Dunand, M.; Seghezzi, C.; Grouzmann, E., Stabilization of urinary biogenic amines measured in clinical chemistry laboratories. *Clinica Chimica Acta* **2021**, *514*, 24-28.
- 49. Boussaad, S.; Tao, N. J.; Zhang, R.; Hopson, T.; Nagahara, L. A., In situ detection of cytochrome c adsorption with single walled carbon nanotube device. *Chem. Commun.* **2003**, (13), 1502-1503.
- 50. Chen, R. J.; Choi, H. C.; Bangsaruntip, S.; Yenilmez, E.; Tang, X. W.; Wang, Q.; Chang, Y. L.; Dai, H. J., An investigation of the mechanisms of electronic sensing of protein adsorption on carbon nanotube devices. *J. Am. Chem. Soc.* **2004**, *126* (5), 1563-1568.
- 51. Artyukhin, A. B.; Stadermann, M.; Friddle, R. W.; Stroeve, P.; Bakajin, O.; Noy, A., Controlled electrostatic gating of carbon nanotube FET devices. *Nano Lett.* **2006**, *6* (9), 2080-2085.
- 52. Gui, E. L.; Li, L. J.; Zhang, K. K.; Xu, Y. P.; Dong, X. C.; Ho, X. N.; Lee, P. S.; Kasim, J.; Shen, Z. X.; Rogers, J. A.; Mhaisalkar, S. G., DNA sensing by field-effect transistors based on networks of carbon nanotubes. *J. Am. Chem. Soc.* **2007**, *129* (46), 14427-14432.
- 53. Yeoman, C. J.; Thomas, S. M.; Miller, M. E. B.; Ulanov, A. V.; Torralba, M.; Lucas, S.; Gillis, M.; Cregger, M.; Gomez, A.; Ho, M. F.; Leigh, S. R.; Stumpf, R.; Creedon, D. J.; Smith, M. A.; Weisbaum, J. S.; Nelson, K. E.; Wilson, B. A.; White, B. A., A Multi-Omic Systems-Based Approach Reveals Metabolic Markers of Bacterial Vaginosis and Insight into the Disease. *Plos One* **2013**, *8* (2).

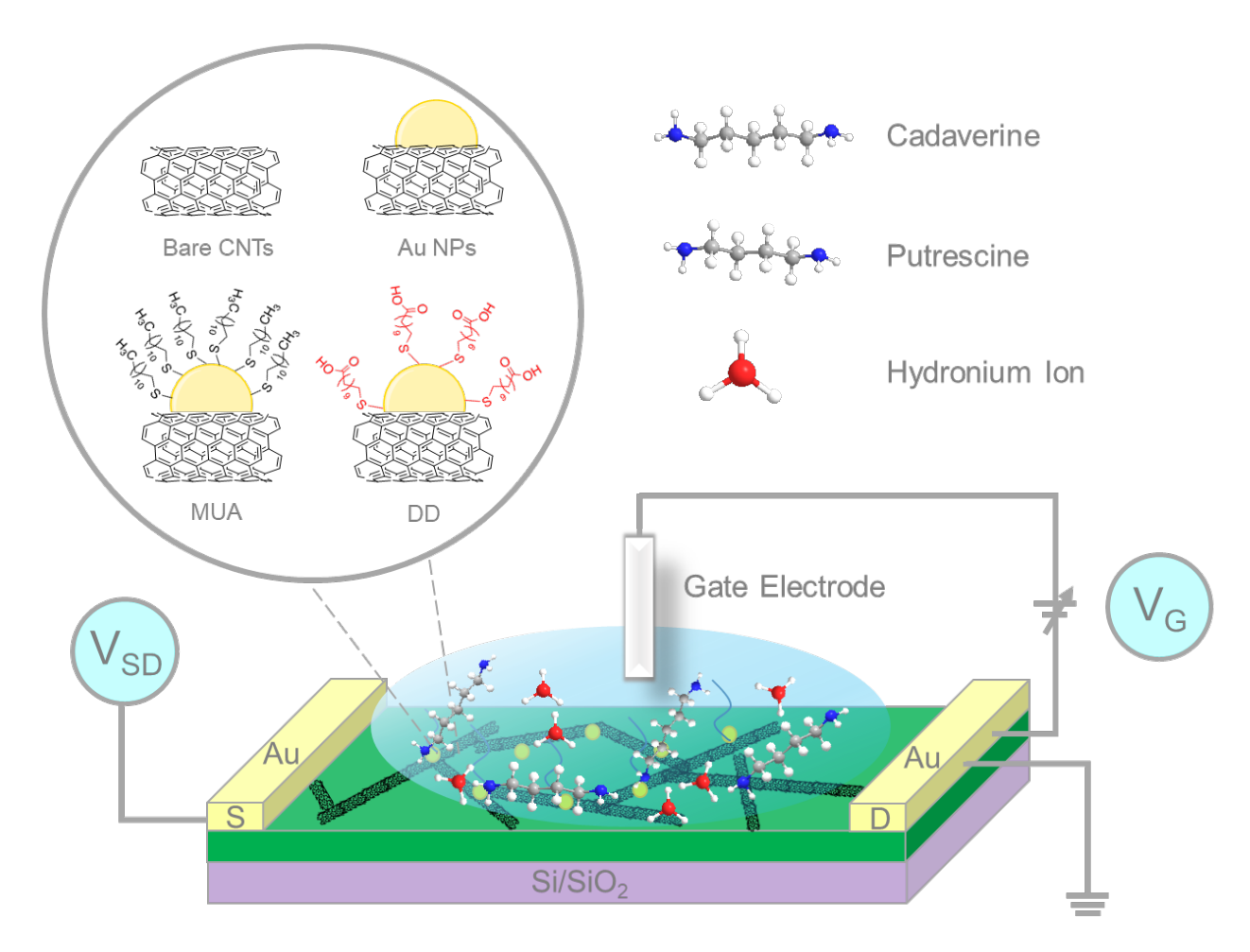


**Figure 1** Schematic illustration of pH/biogenic amine sensing. A 1 M Ag/AgCl reference electrode or a Au reference electrode was employed as liquid gate electrode whereas interdigitated gold electrodes (Gold blocks) were employed as source (S) and drain (D) electrodes with a source—drain bias voltage as 50 mV. The inset shows the different decorations on the carbon nanotubes including bare gold nanoparticles (Au NPs) and gold nanoparticles functionalized with self-assembled monolayers of dodecanethiol (DD) and 11-mercaptoundecanoic acid (MUA). Cadaverine and putrescine are listed as the example of biogenic amines in the graph.

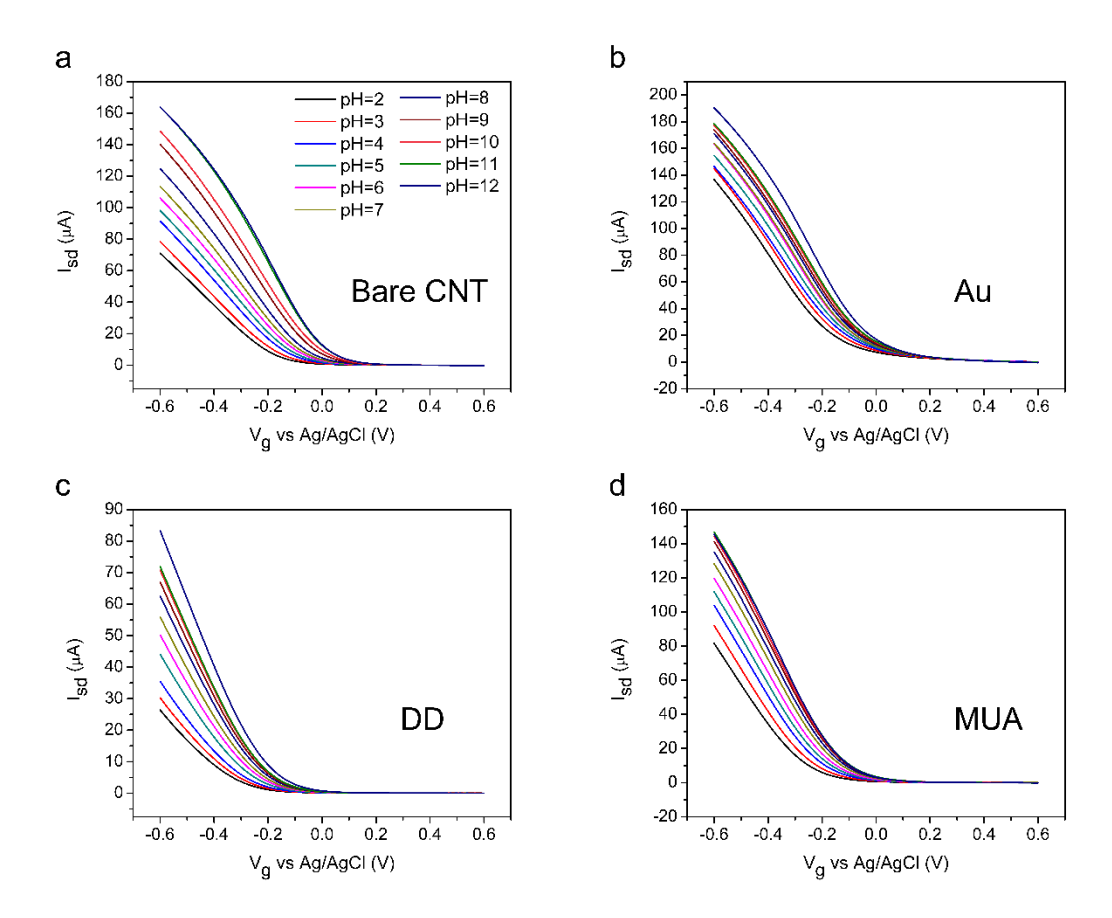


Figure 2 Transfer characteristics of NTFET, i.e, source-drain current ( $I_{sd}$ ) versus applied liquid gate voltage ( $V_g$ ), of NTFET with (a) bare SWCNTs, (b) gold nanoparticles, (c) dodecanethiol, and (d) 11-mercaptoundecanoic acid decoration in the buffers with different pH values from 12 to 2. Drain current was measured by sweepting gate voltage ( $V_g$ ) from -0.6~V to 0.6~V with a source–drain bias voltage ( $V_{sd}$ ) of 0.05~V.

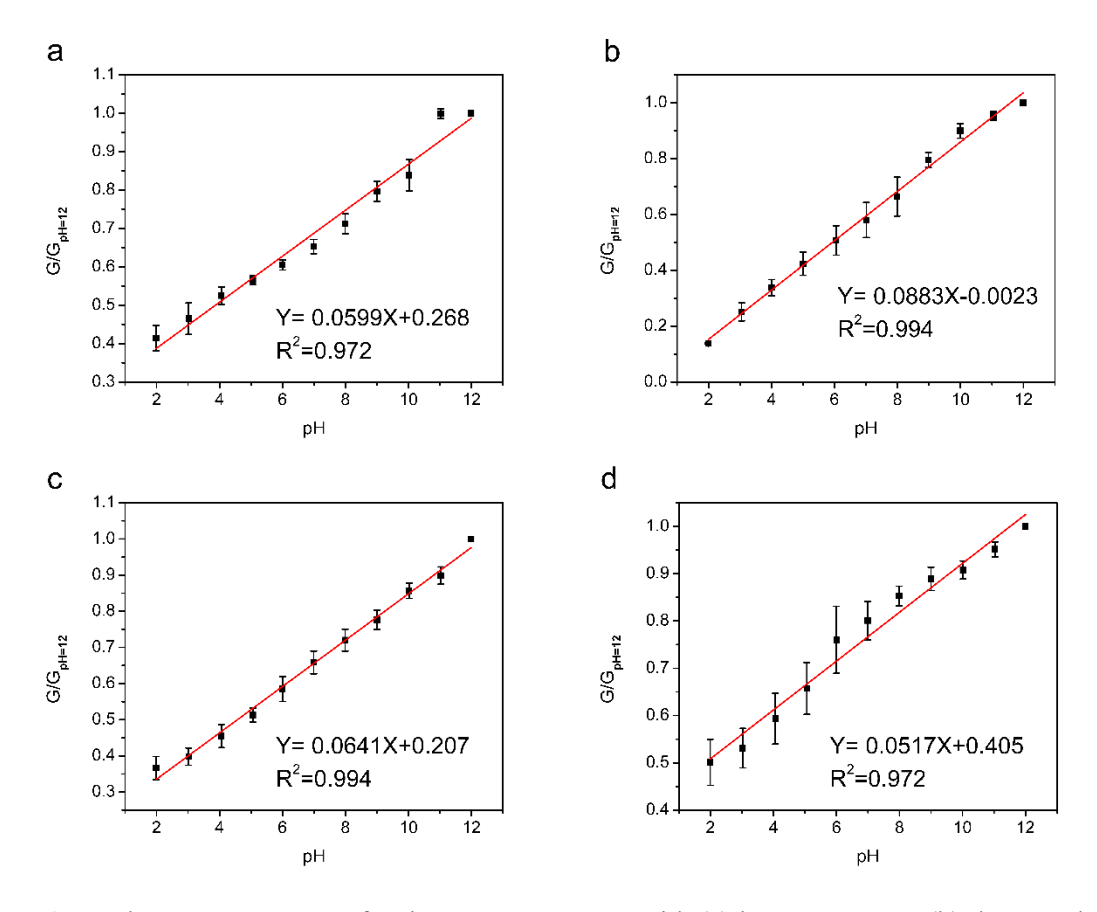
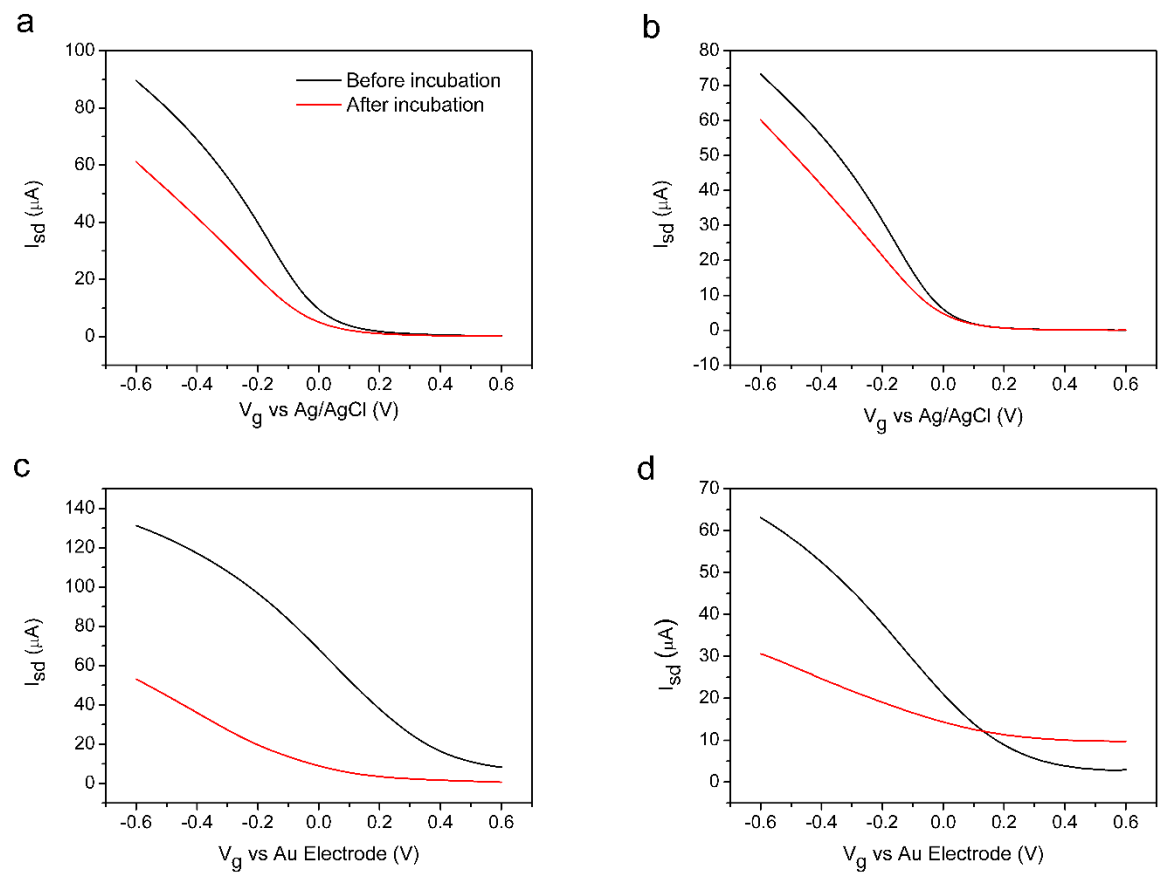
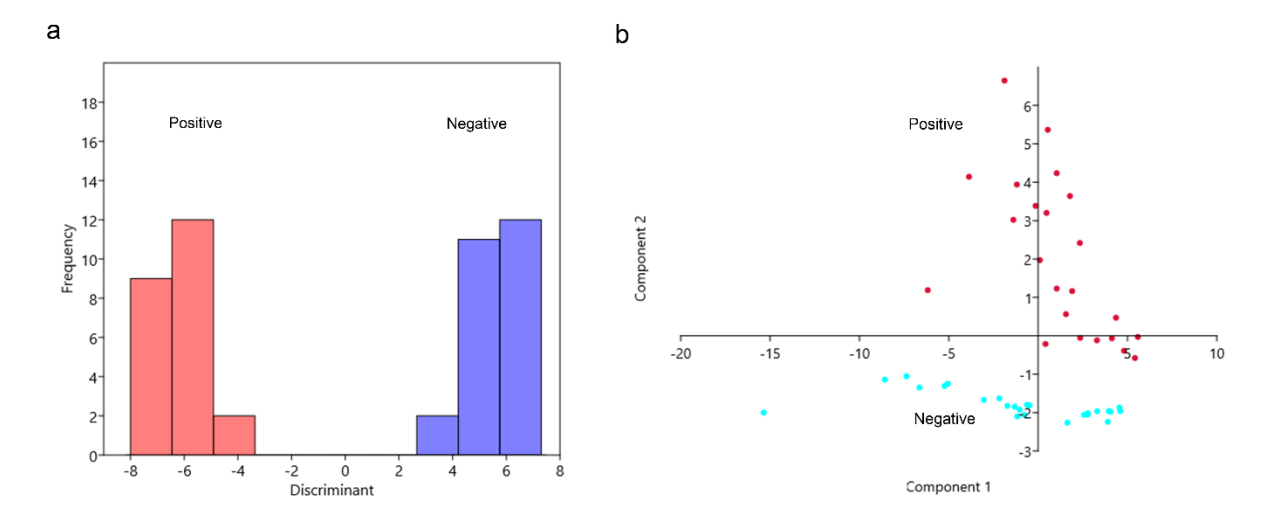


Figure 3 Conductance versus pH for the NTFET sensors with (a) bare SWCNTs, (b) decorated with gold nanoparticles, and after functionalization with (c) dodecanethiol and (d) 11-mercaptoundecanoic acid in the buffers with different pH values from 2 to 12. Source-drain conductance (G) values at  $V_g = -0.5$  V of NTFET devices were normalized to the device conductance ( $G_{pH=12}$ ) in a buffer with a pH of 12. Error bars are calculated with the conductance values of 2 to 4 devices.



**Figure 4** Transfer characteristics of Au-NTFET after incubation with biogenic amines negative (a and c) and positive (b and d) samples. Both Ag/AgCl electrode (a and b) and Au electrode (c and d) were employed as the gate electrode in the measurement. Drain current was measured by sweepting gate voltage ( $V_g$ ) from -0.6~V to 0.6~V with a source–drain bias voltage ( $V_{sd}$ ) of 0.05~V.



**Figure 5** Visualization of training models for the classification of biogenic amine samples with (a) linear discriminant analysis (LDA) and (b) principal component analysis (PCA). The data was collected with a Au electrode as gate electrode in FET measurement.

